Generalized emptying criteria for finite-lengthed capillary

Gopal Verma [1], Chaudry S. Saraj [1,2] Gyanendra Yadav,[3]
Subhash C. Singh,[1,4] and Chunlei Guo [4,*]

[1]*GPL, Changchun Institute of Optics, Fine Mechanics, and Physics, Chinese Academy of Sciences,
Changchun 130033, China*
[2]*University of Chinese Academy of Science, Beijing 100039, China*
[3]*School of Physical Sciences, University of Liverpool, Liverpool L69 3BX, United Kingdom*
[4]*The Institute of Optics, University of Rochester, Rochester, New York 14627, USA*

When a partially filled glass is gently tilted, the liquid can go over its brim without spilling. This happens because of the surface tension and has a direct indication when studying the emptying of a partially filled capillary by modifying the present mathematical criteria of critical emptying. Here, we present an experimental study of the edge effect on emptying a finite-lengthed horizontal capillary, a condition that has never been studied before. We observed that due to the edge meniscus from the finite length of the capillary, critical emptying conditions are significantly altered. Furthermore, by optimizing the edge parameters and the brim wetting effect, water can hold onto much wider capillary brims. We performed numerical simulations using realistic geometries and found excellent agreements with our experimental results. Our results generalize the capillary emptying criterion so that they can be used in realistic geometries and provide guidance in understanding a wide range of phenomena in microfluidics and optofluidics.

Introduction. It is a common experience that slowly tilting a partially filled glass to the horizontal makes the water spill out, and the glass inevitably empties. If we observe it carefully before spilling, the water forms a meniscus at the brim of the glass which prevents water from draining to some extent. In contrast, if the container or tube is narrow enough, such as a drinking straw, the liquid will remain in the container even in the horizontal or inverted position. In his pioneering work [1–3], Finn proposed existence/nonexistence theory for capillary surfaces and obtained specific occlusion criteria for a conducting fluid tube of a given cross section [2]. In Ref. [4], the authors presented an experimental validation of the mathematical criterion for the emptying of a wide rectangular capillary (slit). Recently, this criterion has been extended [5] for capillaries having circular, elliptical, and triangular cross sections.

However, all the cases of capillary emptying presented previously [1–6] consider the length of the capillary (H) to be infinitely long. Hence, the crucial effects of contact line pinning that appeared at the edge of the capillary were disregarded. The wetting [7–10] and spreading [8] processes possess tremendous engineering applications [11–13] and, in spite of it playing a significant role in emptying criteria, the edge effect has received very little attention. The domain of the effect of contact line pinning at the edge of the capillary (edge meniscus) in emptying criteria or (critical width of the capillary, L_c) remains predominantly unexplored. This leads us to investigate the edge effect in the emptying criteria.

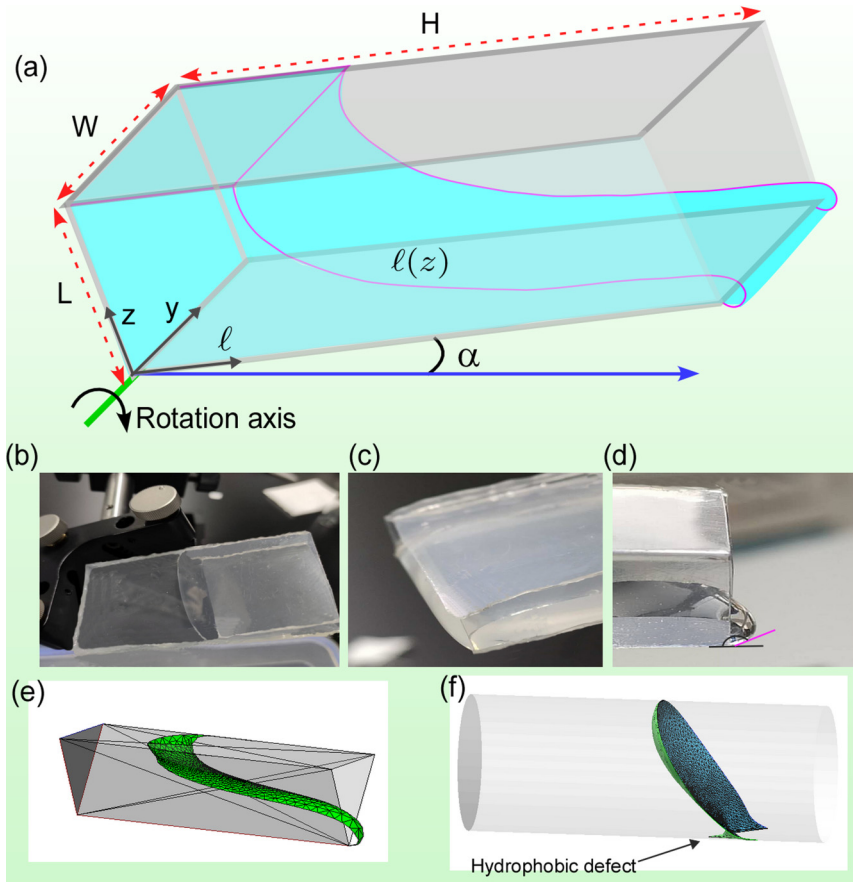*Corresponding author; guo@optics.rochester.edu

FIG. 1. (a) The schematic illustration of the liquid meniscus at the edge of the rectangular capillary. [(b), (c)] Picture of the rectangular capillaries placed on a rotation stage; [(c), (d)] closer picture of the capillary near the edge, while the capillary approaches empty ($\alpha = 0°$); and [(e), (f)] Surface Evolver (SE) simulated images for triangular and circular capillaries.

The main focus in this Rapid Communication is to determine an emptying criterion by including the geometrical edge effect in a finite-lengthed capillary, (H). We showed that due to the edge meniscus in the finite length of the horizontal capillary, the critical emptying criterion is significantly altered, making the water to hold on the edge even in a wider capillary. We also investigated rectangular and triangular capillaries with sharp side edges and observed that due to the edge meniscus, the capillaries can remain filled, which is contrary to the prior predictions that state a capillary will empty at critical value of the opening angle, irrespective of their cross sections. Furthermore, we also investigated the effect of varying in L_c by asymmetrical wetting of the capillary surface through surface texturing or polishing. Interestingly, we observed that structuring modified the contact angle and led to the capillary emptying in a wider range of L_c. Our simulation supports experimental results, and its findings can provide guidance in understanding a wide range of phenomena in microfluidics [13–15] and optofluidics.

Experiments and numerical simulation results. A schematic diagram of our setup is shown in Fig. 1. First, we took a rectangular capillary with a dimension of $L \times H \times W$, having aspect ratio $A_p = W/L$. The capillary was placed on a vibration-free platform in a laboratory-controlled temperature of $T = 20° \pm 1°$. The capillary was initially held vertically before being turned

horizontally. Rotation of the capillary was performed by a rotation stage having $\pm 0.1°$ precision. It is clear that for rotation angle $(\alpha) > 0$, the meniscus adopts a certain shape which minimizes free energy (1). However, for the horizontal capillary $\alpha = 0$, the existence of a meniscus is only guaranteed for sufficiently narrow capillaries. A fast video camera, operating at the speed of 25 to 200 frames/s, was used to record the development of edge meniscus. From the recorded video, we extracted the (i) θ_0, the equilibrium advancing contact angle before liquid touches the edges, and (ii) θ_c, the value of θ at the instant the tongue crosses the edge. In this experiment, monitoring the rate of tongue growth with a radial contact line velocity (0.05 cm/min) was necessary to avoid complications from viscous effects. This was confirmed by stopping the rotation of capillary, whereupon θ_0 remained almost unchanged. The measurements of θ_c, the mean values, were obtained from a tongue profile, photographed approximately at the moment when the tongue was about to cross the edge. The measurements were repeated for several other tongues with the same system.

To validate our experimental data, we first revised the previous [4] emptying line model by including the edge effect. Using a large aspect ratio [$A_p \gg 1$, Figs. 1(b) and 1(c)] capillary or making a round corner in a rectangular capillary, one can reduce the sidewall and side-edge effect [3]. The shape of the meniscus for the tilted capillary can be found by solving the macroscopic free energy per length W [4]: $F[\ell] = \sigma A + g \triangle \rho G + \triangle p V + \sigma S$. Here, σ is the liquid-gas surface tension, $g \triangle \rho$ is the liquid-gas weight density difference, and $\triangle p$ is a Lagrange multiplier. The functional dependence enters through the liquid-gas inter-facial area A, volume V, gravitational contribution G, and $S = -[\cos\theta_0 \, \ell(0) + \cos\theta_L \, \ell(L)]$, where θ_0 and θ_L are the equilibrium contact angle at the upper and lower surfaces of the capillary. For a horizontal capillary ($\alpha = 0$), the minimization of free energy equation leads to

$$1 + \frac{\ell'(z)}{1 + \ell'(z)^2} = \frac{z^2}{2a^2} + \frac{\triangle p}{\sigma} z + (1 - \cos\theta_0), \tag{1}$$

where $\triangle p = \sigma(\cos\theta_0 + \cos\theta_L)/L - (g \triangle \rho L)/2$. The critical emptying condition can be given by Eq. (2) [4]:

$$\frac{L_c}{a} = \sqrt{2(2 - \cos\theta_0 + \cos\theta_L) + 4\sqrt{(1 - \cos\theta_0)(1 + \cos\theta_L)}}, \tag{2}$$

where $a(= \sqrt{\sigma/\rho g})$ is the capillary length. For symmetric capillary $\theta_0 = \theta_L = \theta$, $L_c = 2a\sqrt{1 + \sin\theta}$. It has symmetry and a maximum value of $2\sqrt{2}a$ at $\pi/2$. The maximum value of $L_c(\theta)$ decides the emptying line that separates the filled region (where a meniscus exists) from the empty region (where no meniscus exists). The emptying can be quantified by determining the equilibrium separation between the front and rear parts of the meniscus $\triangle \ell = \ell(z) - \ell(0)$; at $L = L_c$, the tongue height is $z_{L_c} = \sqrt{2(1 - \cos\theta_0)}$ and $\triangle \ell = \infty$. The growth of the tongue in symmetric capillary varies as $\triangle \ell \simeq a \ln(1/\epsilon)$, where $\epsilon = (L_c - L)/L_c$. All the previous theoretical and experimental results considered the H infinitely large to avoid the edge effect [1–6].

If we consider the length of the capillary to be sufficiently small, the continuous tilting of the capillary makes the three-phase contact line meet a sharp edge. Equilibrium condition or pinning regime at a sharp edge is governed by the Gibbs inequality [16–20] condition, $\theta_0 \leqslant \theta \leqslant (180° - \phi) + \theta_0$, where θ is contact angle at the edge of the capillary and ϕ is the angle subtended by the two surfaces forming the capillary edge [Fig. 2(a)]. One of the objectives of this study is to use this inequality in advancing the contact line. By tilting the capillary gently, the liquid layer is forced quasistatically to slowly glide until the triple line touches the edge. We defined θ_c as the critical (upper) value of θ to the moment when the contact line just cross the edge and it becomes $\theta_c = (180° - \phi) + \theta_0$ [16–23]. In terms of the L_c (or the Bond number), Eq. (2) can be rewritten as

$$\frac{L_c}{a} = \sqrt{B_o} = \sqrt{2}[\sqrt{(1 - \cos\theta_c)} + \sqrt{(1 + \cos\theta_L)}]. \tag{3}$$

As the gravity effect becomes dominant, the equilibrium shape of the lower meniscus satisfying the Young-Laplace equation may cease to exist and the liquid falls off before θ_c reaches $180°$ [17,21].
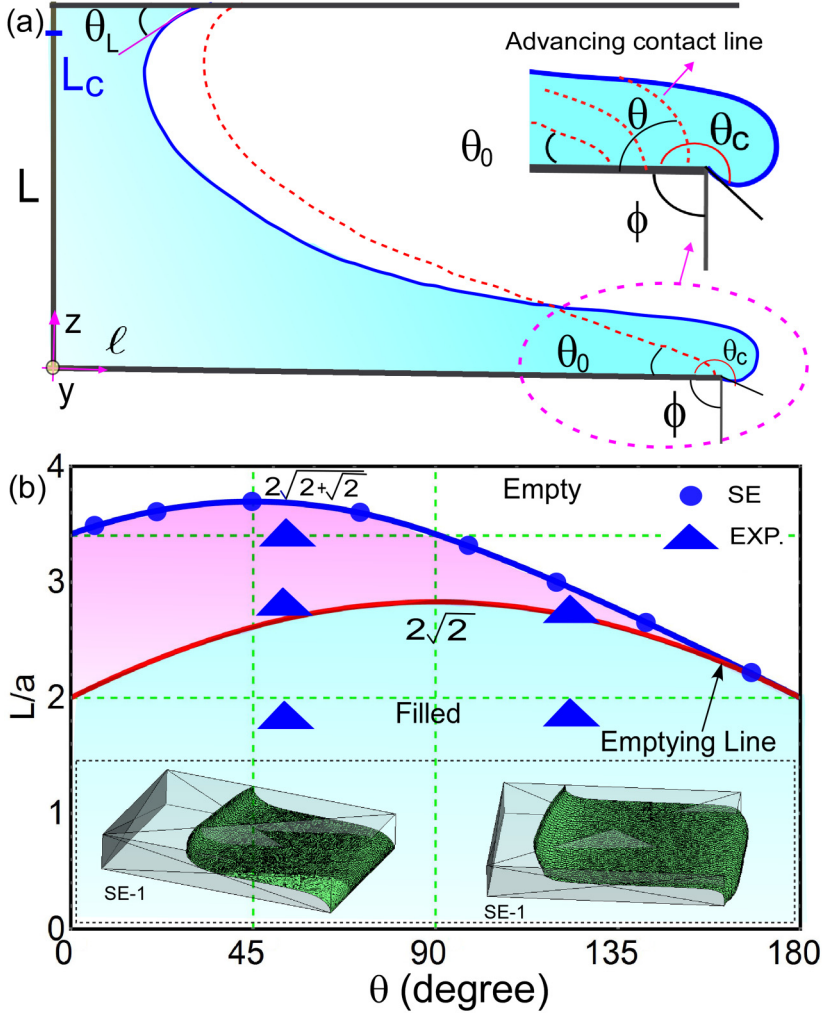
FIG. 2. (a) Schematic of equilibrium of a liquid meniscus at the sharp edge of the capillary. (b) Emptying line for rectangular capillary as a function of contact angle with (red line) and without (blue line) considering the edge effect. Triangles show the experimental data points and size represents an error bar. Blue and red lines are theoretical plots of Eq. (3). SE-1 and SE-2 are simulated meniscus shapes from SE.

Two cases arise depending on the angle between ϕ and θ_0. (i) When, $\theta_0 \leqslant \phi(= 90°)$ such that $\theta_c \leqslant$ 180°, one can see that, when contact angle (θ_0) varies from 0 to 90°, the critical angle (θ_c) varies from 90 to 180°. We examined whether a small tilt of the capillary θ_c induced a contact line beyond the edge. Figure 2(b) shows an emptying line $L_c(\theta_0)$ versus θ_0 from Eq. (3) and experimental data points. We performed an experiment with water in three different capillaries, having widths (L) of 4.5, 6, and 9 mm of two different materials and the contact angles were $\theta_0 = \theta_L = (50°, 120°) \pm 2°$ respectively.

(ii) When, $\theta_0 \geqslant \phi(= 90°)$ and the gravity effect is appreciable, at $\theta = 180°$ and at finite V, the meniscus will eventually tumble over the edge. This is similar to the stability of axisymmetric sessile drops [17], where it has been shown that when the contact line is held at a fixed position, the meniscus will be stable providing $\theta \leqslant 180°$. It means that for $\theta_0 \geqslant 90°$, critical angle (θ_c) for depinning is fixed at 180°. Figure 2(b) shows the plot of Eq. (3) with the experimental data

point. The maximum value of $L_c = 2\sqrt{2 + \sqrt{2}}\, a$ is larger as compared to the previous value of L_c.

We also modeled the capillary emptying with the use of the SE to solve for critical contact angles as well as the shape and horizontal extent of interface ($\bigwedge \ell$) for a given capillary dimension. SE is a geometric minimization code where surfaces and curves are automatically adjusted to locate a minimum of a prescribed functional [6]. We also confirmed the dynamics of meniscus using COMSOL MULTIPHYSICS. The laminar two-phase flow phase-field method was used to solve the Navier-Stokes equation for incompressible flow.

Emptying criteria in circular and triangular capillaries. We also investigated a sharp edge effect in a circular tube and triangular capillary. In Refs. [1–4], authors presented an occlusion and emptying criterion for a capillary with different cross sections. They assumed the *H* and *V* were effectively infinite to prevent the unwanted influence of finite-size effects in their results. In general, the presence of gravity prevents any analytical solution, and hence numerical methods and SE modeling were adopted [2,5,6].

Considering the edge effect, we performed SE simulation to find the emptying line for a circular tube. To do so, for a given R, we tried to get contact angle θ_c by varying the θ_0 until the contact line depinned. After getting the SE data for R_c and θ_0, we fitted these data points with the expression, as in the case of rectangular capillary, $\frac{R_c}{a} = \sqrt{A(A - \cos\theta_c + \cos\theta_R) + B\sqrt{(1 - \cos\theta_0)(1 + \cos\theta_R)}}$, and the fitting parameters are $A = 1$ and $B = 2$. Hence, the expression of R_c becomes

$$\frac{R_c}{a} = \sqrt{[\sqrt{1 - \cos\theta_c} + \sqrt{\cos(\theta_R) + 1}]^2 - 1} \tag{4}$$

where θ_c and θ_R are the contact angles at the edge and remaining contact line attached to the capillary tube.

One can see that critical empty line is modified and has the maximum value $(\sqrt{3 + 2\sqrt{2}})a$, which is larger than without the sharp edge effect [see Fig. 3(a)]. Furthermore, for infinitely long tube, $\theta_0 = \theta_R = \theta$, Eq. (4) gives the critical radius (R_c) values of a and $\sqrt{3}\, a$ for $\theta = 0$ and $\pi/2$ respectively, which is also consistent with previous result [5]. We performed an experiment to find the (R_c) for three different capillary tubes of $R = 3, 5,$ and 6.5 mm and the respective contact angle. These experimental results [Fig. 3(a)] are also consistent with the analytic Eq. (3) and SE simulation.

For triangular capillary, it was predicted [5] that the capillary with an opening angle β will empty for $\theta < (180° - \beta)/2$ and for $\theta > (180° + \beta)/2$, no matter how small the cross section is. We performed experiments with triangular capillaries having $\theta = 45, 65,$ and $85°$ and $\beta = 60° \pm 2°$ [see Fig. 3(b)]. Remarkably, we found that due to the edge meniscus and rounded corner, the capillary does not empty even though $\theta < (180° - \beta)/2$ is satisfied for $45°$. So, in practice it is more realistic to consider an edge as a continuous surface without sharp edge; i.e., it is rounded with radius r_0 [3]. We measured $r_0 = 4.2$ mm for our triangular capillary. Using same procedure as for the circular capillary, we performed SE simulation but we were unable to find out any closed-form analytic equation that can fit with our SE data, as Eq. (4) for circular capillary. The emptying line of a circular and triangular capillaries are included for comparison in Fig. 4 with a dotted line.

Emptying criterion in asymmetrical capillary surface. We showed that the edge effect modified the emptying criteria even in a capillary with the same initial contact angle, $\theta_0 = \theta_L$, owing to the sharp edge induced asymmetry in these contact angles at the edge of the capillary. Several strategies have been used to make hydrophilic and superhydrophobic surfaces [15,23–29]. We consider the hydrophilic and superhydrophobic surfaces to see the effect of contact angle on the critical length L_c. From Fig. 4(c), we can see that the plot of Eq. (3) predicts the following for two different emptying criteria: (a) With $\theta_L \simeq 0$ hydrophilic upper surface and $\theta_0 \simeq 180°$ hydrophobic lower surface, we can achieve maximum value of $L_c = 4\, a$. (b) The microscopic value of $Ł_c = \sqrt{2}a$ can be achieved at $\theta_L = 180°$ for superhydrophobic upper surface and $\theta_0 = 0°$ hydrophilic lower surface. Figure 4 shows the experimental data with numerical and analytical fit [Eq. (3)]. We made the capillary
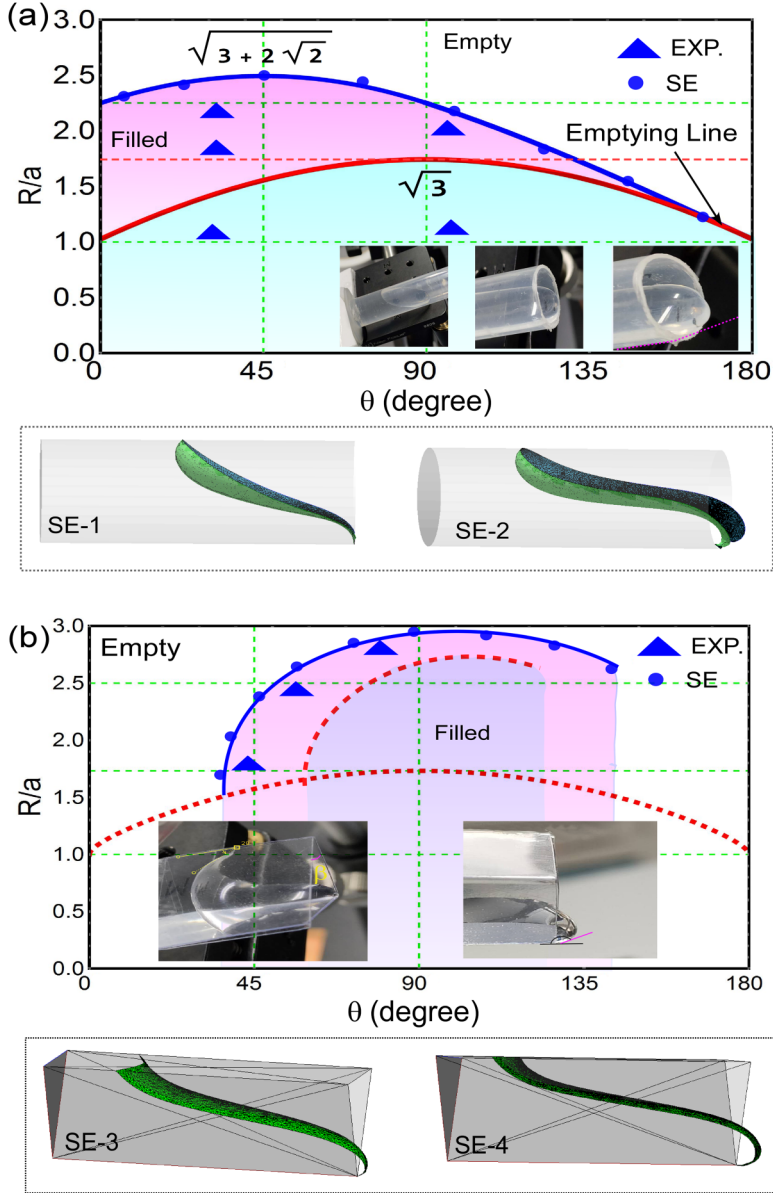
FIG. 3. (a) Equilibrium of a liquid meniscus at the sharp edge of the capillary. (b) Emptying line for capillary tube as a function of θ_0 with (blue line) and without (red line) considering the edge effect. Triangles represent the experimental data points, and their sizes represent error bars. Blue and red lines plot Eq. (4). SE 1–4 are simulated meniscus shapes from SE.

surfaces superhydrophobic by coating wax and micro- and nanostructures using chemical etching. The effect of the asymmetrical wetting provides a wide range of critical widths for emptying criteria, i.e., $\sqrt{2}a \leqslant L_c \leqslant 4a$.

Discussion. The three basic characteristics of the edge meniscus offer potential for diverse applications, First, enhancing the value of the emptying line is useful to sustain liquid in a wider tube. It can also be beneficial in understanding the emptying criteria in other complex-shaped
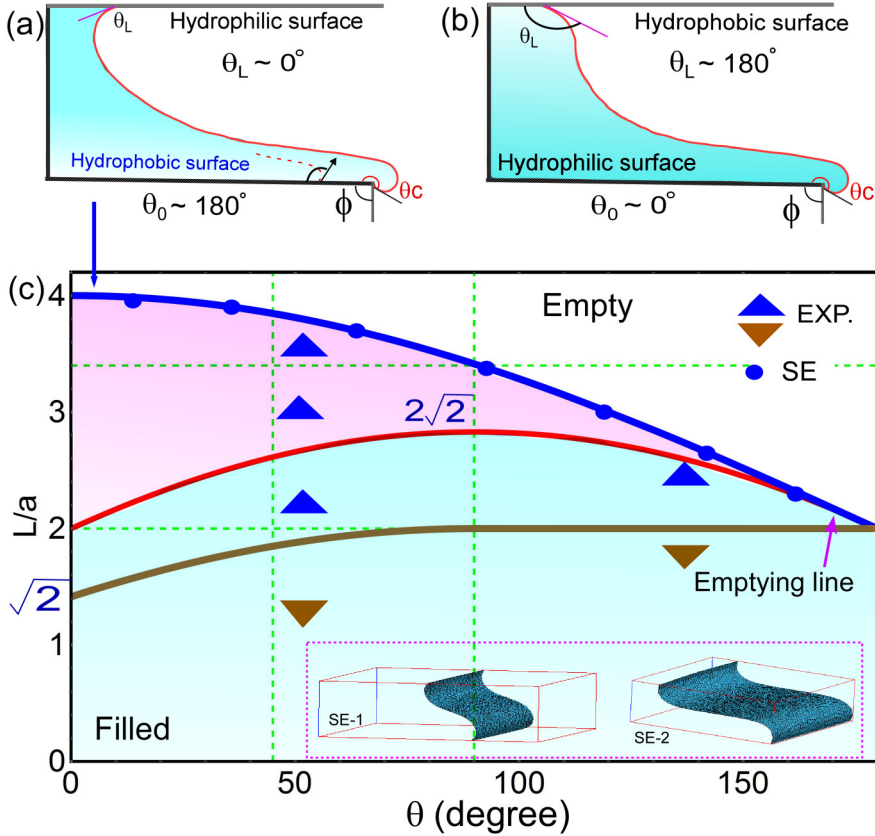
FIG. 4. [(a), (b)] The schematic of hydrophilic and hydrophobic surfaces in asymmetric capillaries. (c) Experimental data with SE simulation; lines represent the Eq. (3) fit. SE-1 and SE-2 are simulated meniscus shapes from SE. Blue line represents the plot of tEq. (3), red line serves as reference for symmetrical capillary, and brown line triangles represent the experimental data points, where their sizes represent error bars.

geometries and localized pinning of contact line by hydrophobic defects etc. Second, in microfluidic [13–15,30,31] devices, the dimension is small and therefore in this case the edge effect is quite vital. In these devices, rapid and efficient handling of a relatively small amount of liquids is possible which is a substantial requirement for molecular biology [12]. Since the critical width (L_c) is directly dependent upon the critical angle, it can be controlled in a reversible manner by altering the critical angle or its wettability [23,24,29,30,32]. Grooved surface topograhy (micro- and nanolithography) can be used for this purpose and various applications [15,33–35]. Electrowetting has also been demonstrated explicitly for the manipulation of contact angle [13]. Last, we showed the effect of rounding the capillary corner on the value of the critical contact angle (emptying line) for the rectangular and triangular capillaries. It is of great significance to know this effect in practice, because it is not easy to fabricate a capillary with a perfectly sharp corner [3]. Hence, one can find the desired L_c by choosing the roundness of the capillary r_0.

In summary, by considering the edge effect, we found emptying criteria that are useful in microfluidic devices [14]. We have demonstrated that we just need to modify the surface properties of the capillary near the edge and the depinning can be triggered by the local behavior at specific features [33–37]. This approach could help the understanding of open problems related to wetting-dewetting transitions, and more broadly the dynamics of free interfaces gliding over solid surfaces, e.g., occlusion [1–3,6], and emptying criteria in other complex geometries.

---

[1] R. Finn, *Equilibrium Capillary Surfaces* (Springer-Verlag, Berlin, 1986).

[2] R. Manning, S. Collicott, and R. Finn, Occlusion criteria in tubes under transverse body forces, J. Fluid Mech. **682**, 397 (2011).

[3] P. Concus and R. Finn, Dichotomous behavior of capillary surfaces in zero gravity, Microgravity Sci. Technol. **3**, 87 (1990).

[4] A. O. Parry, C. Rascón, E. A. G. Jamie, and D. G. A. L. Aarts, Capillary Emptying and Short-Range Wetting, Phys. Rev. Lett. **108**, 246101 (2012).

[5] C. Rascón, A. O. Parry, and D. G. A. L. Aarts, Geometry-induced capillary emptying, Proc. Natl. Acad. Sci. USA **113**, 12633 (2016).

[6] R. E. Manning and S. H. Collicott, Existence of static capillary plugs in horizontal rectangular cylinders, Microfluid. Nanofluidics **19**, 1159 (2015).

[7] P. G. de Gennes, Wetting: Statics and dynamics, Rev. Mod. Phys. **57**, 827 (1985).

[8] D. Bonn, J. Eggers, J. Indekeu, J. Meunier, and E. Rolley, Wetting and spreading, Rev. Mod. Phys. **81**, 739 (2009).

[9] T. Pompe and S. Herminghaus, Three-Phase Contact Line Energetics from Nanoscale Liquid Surface Topographies, Phys. Rev. Lett. **85**, 1930 (2000).

[10] C. Rascón and A. O. Parry, Geometry-dominated fluid adsorption on sculpted solid substrates, Nature (London) **407**, 986 (2000).

[11] N. R. Morrow, Physics and thermodynamics of capillary action in porous media, Ind. Eng. Chem. **62**, 32 (1970).

[12] D. J. Beebe, G. A. Mensing, and G. M. Walker, Physics and applications of microfluidics in biology, Annu. Rev. Biomed. Eng. **4**, 261 (2002).

[13] J. Barman, D. Swain, B. M. Law, R. Seemann, S. Herminghaus, and K. Khare, Electrowetting actuated microfluidic transport in surface grooves with triangular cross section, Langmuir **31**, 1231 (2015).

[14] S.-Y. Teh, R. Lin, L.-H. Hung, and A. P. Lee, Droplet microfluidics, Lab Chip **8**, 198 (2008).

[15] R. Seemann, M. Brinkmann, E. J. Kramer, F. F. Lange, and R. Lipowsky, Wetting morphologies at microstructured surfaces, Proc. Natl. Acad. Sci. USA **102**, 1848 (2005).

[16] J. W. Gibbs, *Scientific Papers* (Dover, 1906; Reprint, 1961), Vol. 1, p. 326.

[17] J. Oliver, C. Huh, and S. Mason, Resistance to spreading of liquids by sharp edges, J. Colloid Interface Sci. **59**, 568 (1977).

[18] L. R. White, The equilibrium of a liquid drop on a nonhorizontal substrate and the Gibb's criteria for advance over a sharp edge, J. Colloid Interface Sci. **73**, 256 (1980).

[19] V. Grishaev, A. Amirfazli, S. Chikov, Y. Lyulin, and O. Kabov, Study of edge effect to stop liquid spillage for microgravity application, Microgravity Sci. Technol. **25**, 27 (2013).

[20] E. Bayramli and S. Mason, Liquid spreading: Edge effect for zero contact angle, J. Colloid Interface Sci. **66**, 200 (1978).

[21] J. Grana-Otero and I. E. Parra Fabián, Contact line depinning from sharp edges, Phys. Rev. Fluids **4**, 114001 (2019).

[22] J. Bostwick and P. Steen, Stability of constrained capillary surfaces, Annu. Rev. Fluid Mech. **47**, 539 (2015).

[23] F. Schellenberger, N. Encinas, D. Vollmer, and H.-J. Butt, How Water Advances on Superhydrophobic Surfaces, Phys. Rev. Lett. **116**, 096101 (2016).

[24] N. Shirtcliffe, G. McHale, M. Newton, G. Chabrol, and C. Perry, Dual-scale roughness produces unusually water-repellent surfaces, Adv. Mater. **16**, 1929 (2004).

[25] A. Y. Vorobyev and C. Guo, Laser turns silicon superwicking, Opt. Express **18**, 6455 (2010).

[26] A. Y. Vorobyev and C. Guo, Multifunctional surfaces produced by femtosecond laser pulses, J. Appl. Phys. **117**, 033103 (2015).

[27] A. Y. Vorobyev and C. Guo, Water sprints uphill on glass, J. Applied Physics **108**, 123512 (2010).

[28] D. Chu, S. C. Singh, J. Yong, Z. Zhan, X. Sun, J.-A. Duan, and C. Guo, Superamphiphobic surfaces with controllable adhesion fabricated by femtosecond laser Bessel beam on PTFE, Adv. Mater. Interfaces **6**, 1900550 (2019).

[29] H. Y. Erbil, A. L. Demirel, Y. Avcı, and O. Mert, Transformation of a simple plastic into a superhydrophobic surface, Science **299**, 1377 (2003).

[30] P. Concus, R. Finn, and M. Weislogel, Measurement of critical contact angle in a microgravity space experiment, Exp. Fluids **28**, 197 (2000).

[31] S. C. Singh, M. ElKabbash, Z. Li, X. Li, B. Regmi, M. Madsen, S. A. Jalil, Z. Zhan, J. Zhang, and C. Guo, Solar-trackable super-wicking black metal panel for photothermal water sanitation, Nature Sustain. **3**, 938 (2020).

[32] T. Kobayashi, K. Shimizu, Y. Kaizuma, and S. Konishi, Formation of superhydrophobic/superhydrophilic patterns by combination of nanostructure-imprinted perfluoropolymer and nanostructured silicon oxide for biological droplet generation, Appl. Phys. Lett. **98**, 123706 (2011).

[33] A. Tuteja, W. Choi, J. M. Mabry, G. H. McKinley, and R. E. Cohen, Robust omniphobic surfaces, Proc. Natl. Acad. Sci. USA **105**, 18200 (2008).

[34] M. L. Blow and J. M. Yeomans, Superhydrophobicity on hairy surfaces, Langmuir **26**, 16071 (2010).

[35] A. Checco, B. M. Ocko, A. Rahman, C. T. Black, M. Tasinkevych, A. Giacomello, and S. Dietrich, Collapse and Reversibility of the Superhydrophobic State on Nanotextured Surfaces, Phys. Rev. Lett. **112**, 216101 (2014).

[36] Y. Lai, X. Gao, H. Zhuang, J. Huang, C. Lin, and L. Jiang, Designing superhydrophobic porous nanostructures with tunable water adhesion, Adv. Mater. **21**, 3799 (2009).

[37] G. Verma and K. P. Singh, Universal Long-Range Nanometric Bending of Water by Light, Phys. Rev. Lett. **115**, 143902 (2015).